

Green synthesis of silver nanoparticles using *Fagopyrum esculentum* starch: antifungal, antibacterial activity and its cytotoxicity

Aparna S Phirange and Sushma G Sabharwal*

Division of Biochemistry, Department of Chemistry, Savitribai Phule Pune University, Pune 411007, India

Received 18 July 2017; revised 15 December 2018; accepted 22 December 2018

Silver nanoparticles (AgNPs) have been synthesized using *Fagopyrum esculentum* starch as a stabilizing and reducing agent. This reaction was carried out in an autoclave at 15 psi, 121°C for 20 min. UV-visible spectrum of the colloidal nanoparticles showed the surface plasmon absorption band with maximum absorbance at 418 nm. Interaction between functional groups present in the starch and nanoparticles were analyzed by Fourier-transform infrared spectroscopy (FTIR). Size of the synthesized nanoparticles was found to be in the range of 20-30 nm, as revealed from transmission electron microscopy (TEM). The X-ray diffraction analysis revealed the face-centred cubic (fcc) geometry of silver nanoparticles. The nanoparticles were found to be good antifungal agents against *Aspergillus niger*. The antibacterial activity of the nanoparticles was also studied. The nanoparticles showed higher inhibitory activity against Gram-negative bacteria (*Escherichia coli*) than the Gram-positive bacteria (*Staphylococcus aureus*). These results thus show that *F. esculentum* starch stabilized AgNPs could be used as a promising antimicrobial agent against bacteria the fungi *In vitro* cytotoxicity assessment of starch stabilized AgNPs has shown no significant cytotoxic effect on human cervical carcinoma cells lines (HeLa) by MTT assay and AgNPs concentration at 200 ug/ml of showed 86% cell viability.

Keywords: Starch, AgNPs, *Fagopyrum esculentum* starch, antimicrobial activity, antifungal activity, cytotoxicity

Introduction

Nanoparticles (NPs) have several applications in the field of catalysis, optoelectronics, chemical sensing, biosensing and biotechnology¹. Considerable attention is being given to metal nanoparticles because they are eco-friendly and have several applications. One of the important considerations in the field of nanotechnology is the development of clean, non-toxic and ecofriendly approach for the synthesis of nanomaterial with a range of sizes and with good monodispersity². Most of the procedures used for the synthesis of metal nanoparticles involve chemical reduction. However, the chemical route that is adopted for the synthesis of various NPs is a potential hazard to health and environment. Currently NPs are mainly synthesized by green synthesis to get large quantities and to reduce the time of synthesis using biomaterials such as glucose, sucrose, maltose, starch, chitosan, hydrocolloid of gum kondagogu and tannic acid. Use of tansy fruit, *Rosa rugosa*, *Cinnamomum camphora*, pine, persimmon, *Ginkgo*, *Magnolia*, *Platanus* and *Phyllanthus* leaf extracts for green synthesis of nanoparticles has also been reported³.

Biomaterials possess internal nanostructures, they are biocompatible and biodegradable hence they are favored over synthetic polymer based materials. In plants starch acts as a major stored energy source and this natural polymer is biodegradable and renewable. Amylose (normally 20–30%) and amylopectin (normally 70–80%) are the two main glucosidic components of the starch^{4,5}. Grinding, sieving and drying are the methods used to extract and refine the starches of plant seeds, roots and stalks by industries. The extracted starch from plants is called “native starch”, and after chemical modifications of native starch it is called “modified starch”. Maize (82%), wheat (8%), potatoes (5%), and cassava (5%) from which tapioca starch is derived are the main sources of starch⁶. Environment friendly reducing and capping agents such as carbohydrates, polysaccharides, alkaloids, flavonoids present in the plant extract plays an important role in case of green synthesis of silver nanoparticles⁷. Buckwheat seeds are used as step food in most of the countries like central Europe, eastern Europe and in some part of Japan⁸. Starch is low cost, environmental friendly, abundant raw material, most probably it is applicable in the preparation of degradable plastics and blend films in different areas like agricultural, medicinal and packaging industries. It is low coat material⁹.

*Author for correspondence:

Tel: +912025696061; Fax +912025691728

ssab@chem.unipune.ac.in, drsushma02@gmail.com

Three main steps are involved in the green synthesis of silver nanoparticles, which must be evaluated based on green chemistry perspectives (1) selection of solvent medium, (2) selection of environmentally benign reducing agent and (3) selection of non-toxic substances for the silver - nanoparticles stability². Silver metal is non-toxic to human cells at very low concentrations. In normal use, non toxicity of silver is established by epidemiological history of silver¹⁰.

Bactericidal behavior of silver nanoparticles is attributed to the presence of electronic effects that are brought about as a result of changes in local electronic structures of the surfaces due to smaller sizes. These effects are considered to be contributing towards enhancement of reactivity of silver nanoparticle surfaces. Ionic silver strongly interacts with thiol groups of vital enzymes and inactivates them. It has been suggested that DNA loses its replication ability once the bacteria are treated with silver ions⁷. Main target of the silver nanoparticles is the plasma membrane of the bacteria so these AgNPs disturb the functions of the ion channels in the plasma membranes of bacteria and therefore significant increase in the permeability of plasma membrane takes place. Also, levels of the intracellular adenosine triphosphate (ATP) get decreased so it causes bacterial cell death¹¹.

In the present work we have focused on green synthesis of silver nanoparticles (AgNPs) using biodegradable raw starch isolated from the seeds of *Fagopyrum esculentum* as a reducing and capping agent as well as antimicrobial activity of the synthesized AgNPs was tested using two bacteria *Escherichia coli* (Gram negative) and *Staphylococcus aureus* (Gram positive) as well as fungus *Aspergillus niger*.

Materials and Methods

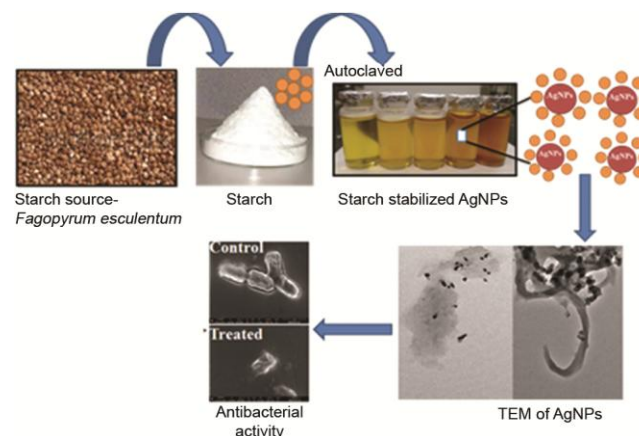
Silver nitrate was purchased from Sisco Research Laboratory, India. Starch was isolated in our laboratory from the seeds of *F. esculentum* purchased locally. *E. coli* and *S. aureus* used for studying the antibacterial activity were obtained from National Collection of Industrial Microorganism (NCIM), National Chemical Laboratory, Pune, India. Luria-Bertani (LB) and potato dextrose agar (PDA) media were supplied by Hi-Media Laboratory, India. *A. niger* used for antifungal activity was isolated in our laboratory and its identification was done at Agarkar Research Institute, Pune, India.

Synthesis of *F. esculentum* Starch Stabilized Silver Nanoparticles (AgNPs)

For synthesis of AgNPs, 0.1% (0.1g w/v) starch was dispersed in 80 ml distilled water by heating it continuously at 80-90°C for 30 min under constant stirring and pH 8 was maintained by using NaOH. To this 20 ml of 1 mM AgNO₃ was added after the temperature of dispersion was brought to room temperature and it was kept in autoclave at 15 psi pressure, 121°C for 20 min¹². Effect of time on synthesis of AgNPs was studied by carrying out synthesis for different time intervals (10, 20, 30 and 40 min) by keeping the starch and AgNO₃ ratio constant. The effect of pH on the synthesis of AgNPs was studied by carrying out reactions at different pH (pH 6, 8, 10, 12 and 14) by keeping the starch and AgNO₃ ratio constant. The effect of concentration of AgNO₃ on nanoparticle synthesis was evaluated by carrying out reactions at different concentrations of AgNO₃ (1 mM–5 mM) where the starch concentration was kept constant at 0.1% (w/v). Similarly the effect of starch concentration on the synthesis of AgNPs was studied by carrying out the reaction at various concentrations of starch (0.1 to 0.5% (w/v)) with the AgNO₃ concentration kept constant at 1 mM. All above parameters were monitored by UV spectrophotometry.

Stability of AgNPs Checked by Iodimetric Titration

The stabilization of AgNPs by starch was analyzed by iodimetric titration. The AgNPs synthesized using *F. esculentum* starch was titrated with iodine solution (0.1N I₂ and 0.1N KI) and at regular intervals the change in color was observed by UV-visible spectrophotometry. When blue color was obtained due to the amylose iodine complex, more AgNPs were added and the spectrum was recorded again¹².



Schem 1— Synthesis of silver nanoparticles from starch.

Characterization

Different techniques used to obtain complementary information about the size and morphology of the starch stabilized AgNPs included UV visible spectrophotometry (Simadzu UV-1800), X-ray diffraction (XRD) using an X-ray diffractometer (Philips PW1710, Holland) with CuK α radiation $\lambda= 1.5405 \text{ \AA}$ over wide range of Bragg angle 10-90 $^{\circ}$ C, transmission electron microscopy (TEM) was done using JEM-3010, Jeol, Japan model. Diffraction light scattering (DLS) and zeta potential was performed to check the particle size, size distribution and shape of the particles (Nano Brook Omni, Brookhaven, New York). The changes in the surface chemical bondings and surface composition were characterized by using fourier transform infrared (FTIR) spectroscopy in the diffuse reflectance mode at a resolution of 4 particles cm^{-1} and samples were prepared in aqueous media without potassium bromide (KBr).

Antibacterial Activity

Bacterial Culture

Antibacterial effect of starch stabilized AgNPs against the bacteria *S. aureus* (NCIM No. 5221) and *E. coli* (NCIM No. 2563) was studied. Both bacteria were cultivated in LB nutrient broth at 37 $^{\circ}$ C for 24 h to get the exponential growth phase. The cells were then harvested and suspended in physiological saline solution (0.85%, NaCl) to maintain the concentration of 107-108 colony forming units per ml (CFU mL^{-1}). The optimal density of bacterial cells was adjusted to 0.5 McFarland standards.

Measurement of Minimum Inhibitory Concentration of AgNPs

To check the antibacterial activity, green synthesized AgNPs were kept for lyophilization and isolated AgNPs were used for further studies. The minimum inhibitory concentration (MIC) of synthesized AgNPs (resuspended 1 mg/ml in distilled water), for *E. coli* and *S. aureus* was determined as follows: different concentrations of nanoparticles (30, 45 and 60 $\mu\text{g/ml}$ for *E. coli*) and (90, 105 and 120 $\mu\text{g/ml}$ for *S. aureus*) were added to 2 ml LB broth. To this 10 μL bacterial cells (107-108 CFU mL^{-1}) were added and the mixture was incubated at 37 $^{\circ}$ C. The bacterial growth was monitored by measuring optical density (OD) at 600 nm after 2 h time interval. Corresponding positive control containing AgNPs, LB broth devoid of inoculum and a negative control containing innoculum, LB broth, devoid of AgNPs were also incubated simultaneously. Minimum inhibitory concentration (MIC) is defined as the lowest concentration of material that inhibits the growth of an organism.

Cell Viability Test of Bacteria

The antibacterial activity of the AgNPs was investigated with the help of cell viability test for *E. coli* and *S. aureus*, using colony count method as follows: 10 μL cells were added into 2 ml of the test solution containing different concentrations of the isolated AgNPs (for *E. coli* - 30, 45 and 60 $\mu\text{g/ml}$ and for *S. aureus* - 90, 105 and 120 $\mu\text{g/ml}$). These AgNPs treated samples were incubated at 37 $^{\circ}$ C with *E. coli* and *S. aureus* for 4 h under shaking conditions. Above mixtures were diluted with a gradient method and spread on LB agar plates. The plates were incubated for 24 h at 37 $^{\circ}$ C. Bacterial growth inhibition was calculated by counting colonies in AgNPs treated cells and compared to those on control plates. All treatments were prepared in duplicate and repeated at least thrice to check the reproducibility.

Loss of viability was calculated using the following equation

$$\text{Bacterial growth inhibition \%} = \frac{C_c - C_s}{C_c} \times 100$$

Where, C_c -Colony count of control cells and C_s -Colony count of treated cells

Antifungal Activity of Starchstabilized AgNPs

The effect of nanoparticles on the fungus *A. niger* was studied using varying concentrations of the AgNPs and evaluating the inhibition of fungal growth, by colony count method and reduction in mycelium dry weight in presence of the AgNPs as compared to control devoid of the AgNPs. The changes in the morphology of AgNPs treated mycelia were examined by scanning electron microscopy (SEM).

Inoculum Preparation

A. niger was isolated in our laboratory. The fungi were grown on PDA plates and the plates were incubated at 35 $^{\circ}$ C for 4 days. The mycelia collected from 4 days old culture were suspended in 10 ml of sterile distilled water. The suspension was stirred on vortex and used for counting the number of cells per milliliter by haemocytometer.

Measurement of Minimum Inhibitory Concentration (MIC)

The fungal growth inhibition was studied by initially determining the MIC as follows: 20 μL of the fungal conidial suspension (5×10^4 cells/ml) was added to 2 ml of potato dextrose broth (PDB) containing varying concentrations of nanoparticles (30, 60, 90, 120 and 150 $\mu\text{g/ml}$) and incubated at 35 $^{\circ}$ C for 24 h. Fungal growth was monitored by

determining the absorbance at 600 nm on a spectrophotometer after every 2 h. MIC was determined and percent growth inhibition as compared to control was calculated.

Cell Viability Test of Fungi

To determine fungal growth in presence and absence of AgNPs, cell viability test was carried out as follows: Varying concentrations of nanoparticles (30 to 120 µg/ml) was added to 20 ml of PDB containing 0.1 ml cell suspensions (5×10^4 cells/ml) of the fungi in conical flasks and the mixture was incubated at 35°C for 48 h. Corresponding controls devoid of AgNPs were run simultaneously. After 48 h, 20 µl of the broth was spread on PDA plate. The plates were kept at 35°C for 48 h and inhibition of growth as compared to control and the number of colonies was calculated.

Determination of Dry Weight

The AgNPs treated and control fungal mycelia were incubated for 7 days in PDB at 35°C essentially as described above. After 7 days, all samples were centrifuged at 4000 rpm for 10 min, washed with distilled water and kept for drying on weighed filter paper (Whatman No. 1) strips at 80°C for 8 h. The filter paper strips containing the dry mycelia were weighed. Percent growth inhibition was calculated by measuring the dry weight of treated and control mycelia as per formula of Sharma and Tripathi¹³

$$\{\% \text{ Growth Inhibition}\} = \frac{C_w - S_w}{C_w} \times 100$$

Where, C_w represents weight of control (untreated) mycelia and S_w represents weight of NP treated mycelia.

Scanning Electron Microscopy (SEM)

The morphological changes in the control and AgNPs treated bacterial and fungal cells were examined by SEM as follows: Fungal mycelia or the bacterial cells were fixed in glutaraldehyde (2.5% v/v phosphate buffer, pH 7.2) and dehydrated by sequential treatment with 50, 60, 70, 80, 90, 95 and 100% ethanol for 15 min. The dried mycelia or bacterial cells were sputter-coated with platinum for SEM imaging.

Cytotoxicity Assay

MTT {3-(4, 5 dimethylthiazol-2-yl)-2,5 diphenyltetrazolium bromide} Assay

Cytotoxicity evaluation of starch stabilized silver nanoparticles was performed as described Ghosh *et al*¹⁴.

Approximately 1×10^5 per ml cells (HeLa cell lines) in their exponential growth phase were seeded in a flat bottomed 96 well polystyrene coated plate and incubated for 24 h at 37°C in a CO₂ incubator. Various dilutions (6.25, 12.5, 25, 50, 100, 200 µg/ml) of aqueous AgNPs in the Dulbecco's modified eagle medium (DMEM) was added to the plate containing trypsinized HeLa cell cultured in complete DMEM media. After 24 h of incubation, 100 µl MTT reagent was added to each well and was further kept for 4 h incubation. Formazan crystals formed after 4 h in each well were dissolved in 100 µl of detergent and the plates were read immediately in a microplate reader at 570 nm. Wells with complete medium, nanoparticles and MTT reagent without cells were used as blanks. Untreated HeLa and treated cells with silver nanoparticles for 24 h were subjected to the MTT assay for cell viability determination.

Results & Discussion

However, in most of the cases, materials and process involved are either expensive or time consuming. Silver, being highly electropositive, is easy to reduce to zero valence from its Ag⁺ oxidation state. Various reducing agents such as borohydrides, aldehydes, sugars and alcohols including polyols have been used to reduce Ag⁺ to Ag⁰. Sugars and alcohols are processed components but buckwheat starch is raw material which we have used for this study as a reducing agent. This study represents the green synthesis of AgNPs from biodegradable reducing agent (buckwheat starch) as well as acting as a capping agent and evaluating the antibacterial and antifungal activity of the synthesized AgNPs.

UV-visible spectroscopy is one of the most widely used techniques for structural characterization of AgNPs. The shape of the spectra gives preliminary information about the size and the size distribution of the AgNPs¹⁵. The absorption spectrum (Fig. 1A) of the pale yellow silver colloids prepared by reduction showed a surface plasmon absorption band at 418 nm. Similar absorption peak was observed in earlier reports for silver nanoparticles synthesized using gum kondagagu¹⁶ and locust bean gum¹⁷. Different parameters which affect the synthesis of AgNPs were optimized these included the time of synthesis, the concentrations of starch and AgNO₃, relative ratio of amounts of starch and AgNO₃ and the pH at which the reaction was carried out.

As seen in Figure 1A, AgNPs were prepared with using different concentrations of AgNO₃ and at higher concentration of AgNO₃ agglomeration of AgNPs was observed where the starch concentration was kept

constant (0.1% w/v). It is observed that absorption intensity was increased with the increasing concentration of AgNO_3 . Similar effects were also observed at pH 10 and above (Fig. 1B), pH 8 was found to be optimal for the synthesis of the AgNPs. At pH 8 is favourable for synthesis of AgNPs and at pH 10 and 12 AgNPs was formed but the NPs are not stable at alkaline pH.

As seen in Figure 1C the optimal concentration of starch for synthesis of the nanoparticles was found to be 0.1%. Absorption peak of AgNPs at 0.3% and 0.4% starch solution was not significant. Absorption intensity increases as the concentration of starch is increases as a reducing and capping agent. But it is found to decrease with increased concentration of starch and no significant effect on SPR intensity and shift. Nucleation might be finished after certain time¹⁸. It indicates that higher concentration of starch strongly acting as a capping agent and nanoparticles are deeply embedded in the viscous polymer matrix. These conditions are not favourable for the interaction of nanoparticles with light. At high concentration of starch, viscosity of solution is high because of this reason functional groups of biopolymer starch are not exposed or polymer chains are not freely expanded and not readily available for the reduction of Ag^+ to Ag^0 .

The effect of relative ratio of volumes of starch (0.1%) and AgNO_3 (1 mM) on AgNPs synthesis was studied by varying the volume of starch and keeping the volume of AgNO_3 constant. As seen in Figure 1D,

agglomeration of nanoparticles was decreased when the volume of starch was increased (1:1 to 1:5). There is no agglomeration at 1:5 ratio was observed while at 1:4 ratio slight agglomeration was seen. To determine the all parameters for synthesis of AgNPs, ratio of volume of AgNO_3 : starch (1:5) was kept constant through out the synthesis.

UV-visible absorption spectra of AgNPs obtained by autoclaving the reaction mixture for different times (5 to 40 min) is shown in Figure 1E. The intensity of the peak of AgNPs was found to increase with increase in reaction time, upto 20 min, which can be attributed to increased reduction of Ag^+ to Ag^0 . However, no significant increase in absorption intensity was observed on increasing the time of autoclaving above 20 min indicating the completion of reaction within 20 min¹⁸.

The AgNPs were prepared by using a basic solution (pH 8) of starch 0.1% and 1 mM AgNO_3 in 1:5 (AgNO_3 : starch) proportion and kept in autoclave for 20 min. Figure 2 shows the spherical morphology of AgNPs by TEM analysis. Size of the AgNPs was calculated by ImageJ software and it was found to be in the average range of 20-30 nm.

The FTIR spectra of native starch and starch stabilized AgNPs were recorded to identify the functional groups which are involved in the reduction of Ag^+ to Ag^0 and to stabilize the nanoparticles (Fig. 3). The broad bands observed in both starch and AgNPs at 3243 and 3309 cm^{-1} can be assigned to stretching vibrations of -OH groups. It shows these

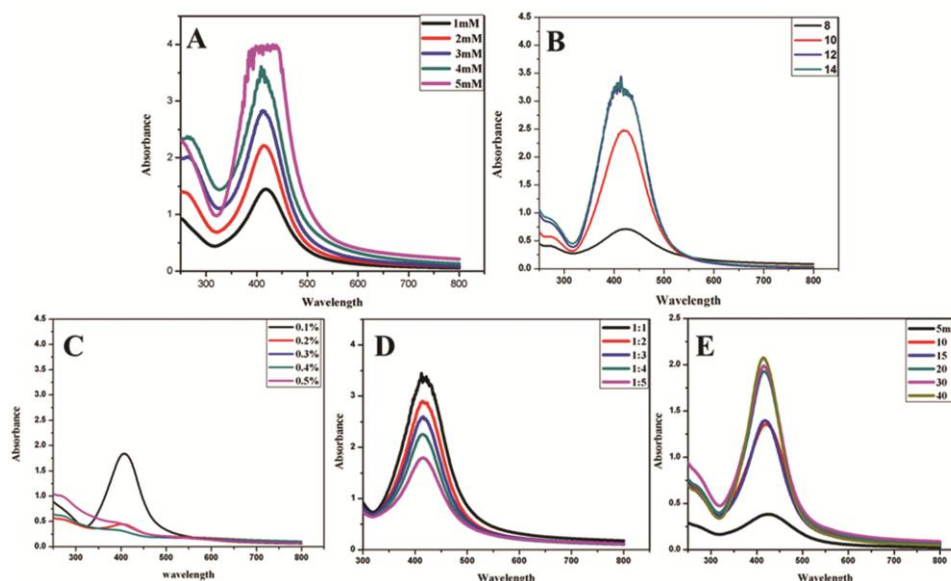


Fig. 1 — Effect of (A) AgNO_3 concentration and (B) pH on the synthesis of nanoparticles, (C) Starch concentration, (D) Ratio of volume of starch and AgNO_3 and (E) Time on the synthesis of AgNPs.

hydroxyl groups are involved in the synthesis of nanoparticles. Band at 2935 cm^{-1} may correspond to the methyl C–H asymmetric stretching or aldehyde (–CHO) respectively. One additional band found at 2320 cm^{-1} in native starch FTIR but not in the AgNPs spectra can be assigned to carbonyl groups (C=O) in native starch. Prominent peak observed at 1733 cm^{-1} in starch which shifted to 1741 cm^{-1} in AgNPs can be assigned to

carboxyl group (COOH). In IR spectra of nanoparticles a shift in the absorbance peaks was observed from 3243 to 3309 cm^{-1} , 1733 to 1747 cm^{-1} and 1000 to 1016 cm^{-1} . This change in shape and shifting observed in nanoparticle peaks suggests the involvement of –OH and –COO groups in the synthesis of AgNPs¹⁹.

In the XRD spectrum (Fig. 4) the broad reflection at 2θ is due to the low crystallinity of the starch

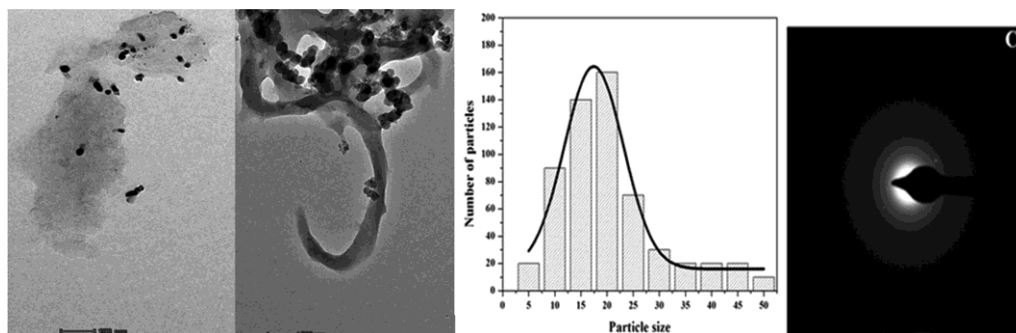


Fig. 2 — (A) TEM, (B) Particle size distribution and (C) SAED pattern.

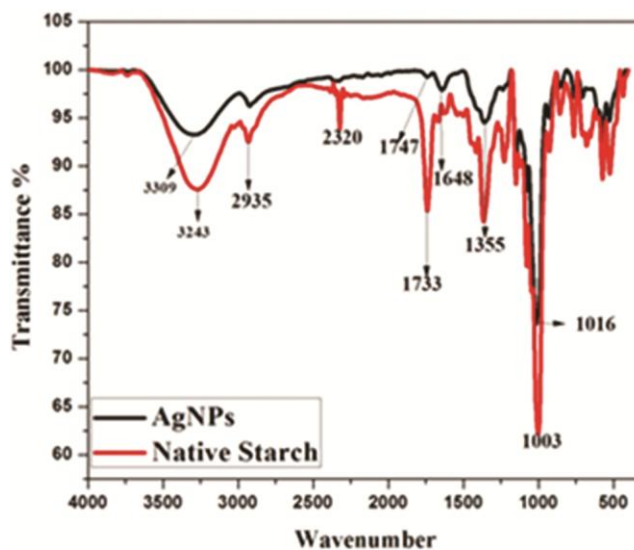


Fig. 3 — FTIR of silver nanoparticles (black line) and native starch (red line).

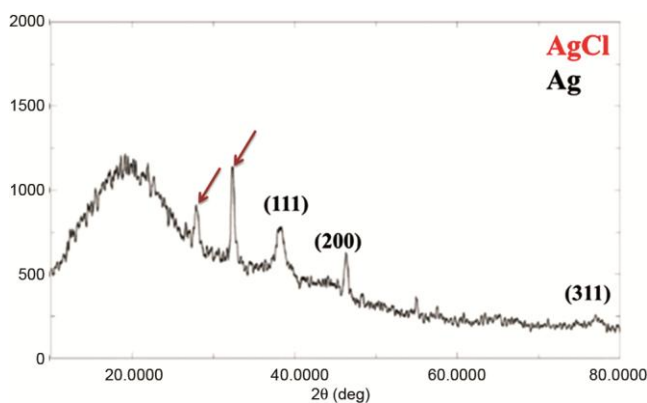


Fig. 4 — X-ray diffraction pattern of silver nanoparticles.

and presence of high amylose crystals; similar observations are reported in the literature^{12,20} and AgNPs showed six intense peaks²¹ but the prominent peaks for silver at $2\theta = 38.13^\circ, 44.21^\circ, 64.47^\circ, 77.37^\circ$, represents the (1 1 1), (2 0 0), (2 2 0), (3 1 1) and (2 2 2) Bragg's reflections of the face-centered cubic structure (JCPDS file: 03-0931) of silver and XRD is existing extra peaks of AgCl nanoparticles at $27.9^\circ, 32.3^\circ, 46.3^\circ$ (JCPDS file: 31-1238) according to Duran *et al*²² or may be those extra peaks due to presence of bioorganic material in starch²¹. The size of the Ag nanoparticles was also determined from X-ray line broadening using the Debye-Scherrer formula given as $D = 0.9\lambda/\beta\cos\theta$, where D is the average crystalline size (\AA), λ the X-ray wavelength used (nm), β the angular line width at half maximum intensity (radians) and θ the Bragg's angle (degrees). For (1 0 1) reflection at $2\theta \approx 38.13$, for $\beta = 0.367200$ radians, $\lambda = 1.54\text{\AA}$ and $\theta \approx 19.06$, the average size of the Ag nanoparticles was 10-25 nm.

Dynamic light scattering (DLS) analyses the size distribution profile of the nanoparticles in a polymer solution. DLS also measures the hydrodynamic diameter and polydispersity of the molecules or nanoparticles. Based on the TEM results range of the size of the nanoparticles was found to be 20-30 nm. Fe-starch capped Ag nanoparticles showed an average hydrodynamic diameter of 189.56 nm and polydispersity was 0.266. As expected size of the AgNPs is larger than the TEM size. As it has been mentioned previously, TEM sizes were similar to XRD measurements, while the DLS sizes were

significantly larger than both. TEM measures only the number based size distribution and does not include the capping agent, while DLS measures the hydrodynamic diameter which includes diameter of the particles, plus ions or molecules attached to the surface²³.

The benchmark of stability of NPs are considered when the values of zeta potential is in the range of +30 mV to -30 mV. Surface zeta potentials were measured using the laser zeta meter (Nano Brook Omni, Brook-haven, New York). Liquid samples of the nanoparticles (3 ml) were diluted with distilled water. The zeta potential was measured after equilibration of solution to find out the surface potential of the silver nanoparticles. Average of three separate measurements was considered, which was -37.75 and it is close to the standard values of zeta potential of NP²⁴.

The UV-vis spectra of AgNPs recorded at different time intervals after addition of iodine (0.1N $I_2 + 0.1N$ KI) solution suggest that AgNPs are present inside the helical structure of the amylose chain (Fig. 5). The AgNPs gave a peak at 418 nm (Fig. 5A) while pure iodine and silver iodide complex produced peaks at 290, 355 nm, respectively (Fig. 5D). When iodine was added to starch stabilized AgNPs, silver iodide was initially formed and peak was obtained at 425 nm (Fig. 5B). Excess addition of iodine gave a peak at 585, 355 and 425 nm (Fig. 5E). This deep blue color was due to the complex formation of I_3^- and amylose. Further addition of excess AgNPs attracted the iodine from the complex resulting in the formation of a peak

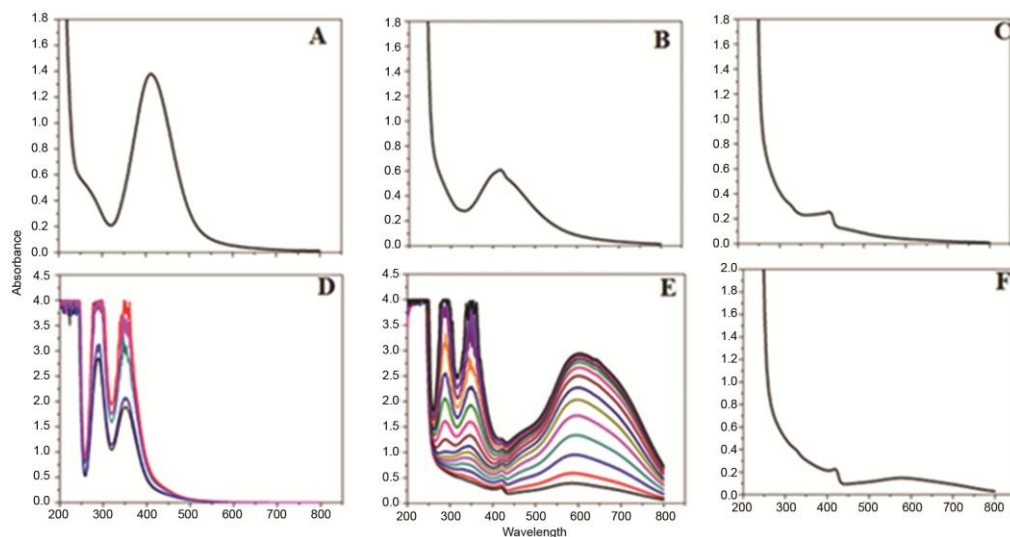


Fig. 5 — UV-vis spectra of (A) Silver nanoparticles; (B) Initial stage after addition of iodine; (C) formation of AgI complex; (D) Iodine; (E) formation of amylose-iodine complex; and (F) addition of excess silver nanoparticles resulting in the formation of AgI complex.

at 425 nm and elimination of the peak at 585 nm (Fig. 5F). These results confirmed that starch is acting as a capping agent for AgNPs.

Antibacterial Activity of AgNPs

Analysis of antibacterial activity of AgNPs was studied using *E. coli* and *S. aureus*. This was done by studying the growth profile of *E. coli* and *S. aureus* and by colony count method. Bacterial cell concentration was adjusted to 10^7 - 10^8 CFU mL⁻¹. Growth profile of bacteria was observed by inoculating the bacterial cells in 1 ml of liquid broth containing AgNPs of different concentrations (30, 45, 60, 75, 90, 105 or 120 µg/ml) and the mixture was incubated at 37°C. Bacterial growth was monitored at 600 nm at different time intervals (Fig. 6). Corresponding controls without AgNPs were run simultaneously for both the bacteria.

In case of *E. coli*, complete growth inhibition was observed at 60 µg/ml concentration of AgNPs. The static bacterial growth was observed at 30 µg/ml concentration of the nanoparticles as compared to control i.e around 90% inhibition was observed. MIC value of NPs for *E. coli* was found to be 60 µg/ml.

In case of *S. aureus*, growth of the bacteria was completely inhibited in presence of AgNPs at a concentration of 120 µg/ml. However, concentration of the AgNPs at 90 µg/ml growth was observed after 10 h of incubation. MIC was found to be 120 µg/ml.

Both bacteria were treated with different concentrations of AgNPs (30 to 120 µg/ml) for 4 h in saline and corresponding controls were run simultaneously. Treated and control samples were plated on LB agar plates with respective dilutions at intervals of one hour till the 4 h and complete inhibition of both bacterial was observed at 2 h incubation. Plates were kept for incubation at 37°C for 24 h. After incubation colonies were counted in treated and untreated samples for both bacteria and growth inhibition was determined. As seen in Figure 7, a significant reduction in colony count was observed after 2 min treated plate as compared to control.

These results reveal that the green synthesized starch stabilized AgNPs exhibited excellent antibacterial activity against *E. coli* (Fig. 7A) at lower concentration (60 µg/ml) with almost 99% inhibition

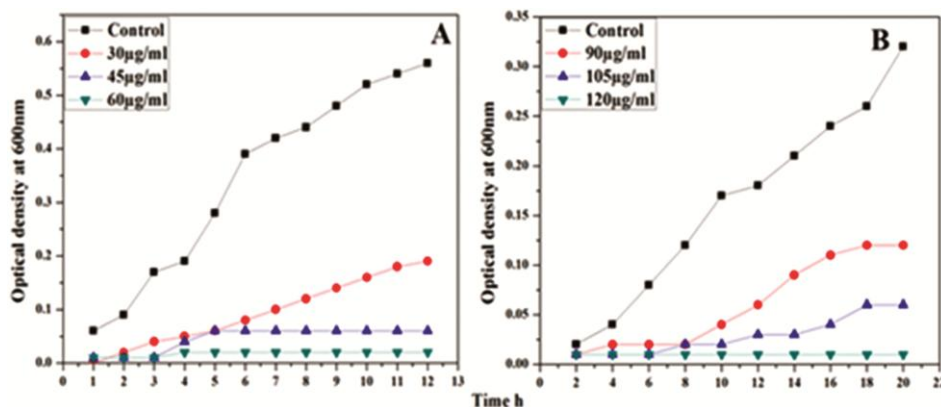


Fig. 6 — Batch growth profiles of (A) *E. coli* and (B) *S. aureus*.

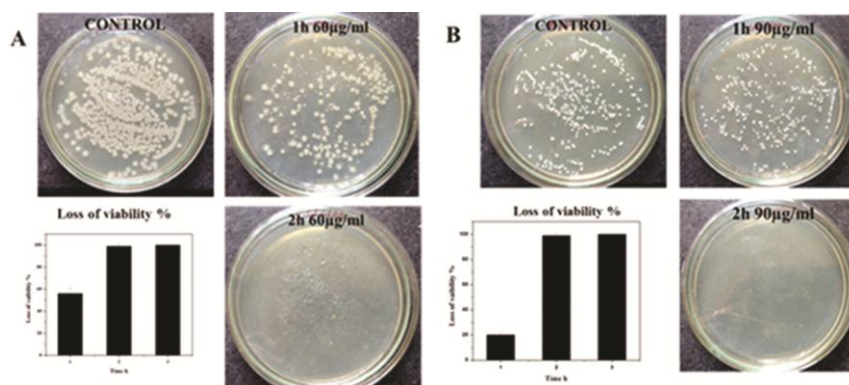


Fig. 7 — Loss of viability of (A) *E. coli* and (B) *S. aureus* calculated by counting colonies.

of growth at this concentration. However, in case of *S. aureus* 90% cell viability loss was observed at a concentration of 90 $\mu\text{g/ml}$ of nanoparticles and a concentration of 120 $\mu\text{g/ml}$ of AgNPs was required for 99% growth inhibition (Fig. 7B). These investigations clearly suggest that the AgNPs were found to be more effective bactericidal agents against Gram-negative bacteria (*E. coli*) than the Gram-positive cells (*S. aureus*). Silver ions cannot easily penetrate the cell-wall due to thicker peptidoglycan layer of cell-wall of Gram positive bacteria than the Gram-negative bacteria which is protecting the cell from penetration of silver ions into the cytoplasm²⁵. This may be due to increased interaction of the nanoparticles with the cell-wall of Gram-negative bacteria, facilitated by the relative abundance of negative charges on the cell wall. The positively charged silver ions interact with cell-wall and get entry inside the cell. Hence growth of Gram-negative bacteria was more profoundly affected by the AgNPs than that of the Gram-positive bacteria²⁶.

In the previous study others have reported antibacterial activity of AgNPs against *E. coli* cells. They observed growth inhibition at around 100 $\mu\text{g/ml}$ of AgNPs after 24 h. They carried out a comparative study on the effects of AgNPs of different shapes and sizes on *E. coli*.^{10,11} They found that spherical and triangular shaped AgNPs showed significant bactericidal effect. In the present study, green synthesis of AgNPs (20-30 nm) has been carried out using starch isolated from *F. esculentum* seeds and screening of their antimicrobial effect on the growth of *E. coli*, *S. aureus* and *A. niger* has been done.

Scanning Electron Microscopic Studies of the Biocidal Effects of AgNPs

Biocidal effects of the synthesised AgNPs on the bacteria (*E. coli* and *S. aureus*) were also studied using SEM. As seen in the SEM micrograph (Fig. 8) the synthesised AgNPs not only adhered to the bacterial cell wall surface, but also penetrated inside the bacterial cells. The nanoparticles completely disturb the biological process of the bacteria, the membrane morphology was also affected due to which the nanoparticles were able to enter inside the cell. This may have caused leaching of ions out of the cell affecting the proton motive force resulting in cell death.

In both *E. coli* (Fig. 8A) and *S. aureus* (Fig. 8B), even at lower concentrations of AgNPs (30 and 90 $\mu\text{g/ml}$) after 4 h treatment, the cell wall of the treated

cells was distorted as compared to control. It has been suggested that Ag ions released from AgNPs may bind with DNA. This may be leading to loss of replication ability of DNA due to Ag ions disordering its helical structure by cross linking the nucleic acid strands. Also, some other cellular proteins and enzymes essential for ATP production may be inactivated^{10,28}. In a previous report on the bactericidal activity of AgNPs, it was shown that the interaction between AgNPs and constituents of the bacterial membrane caused structural changes in cell membranes damaging it and finally leading to cell death^{26,29-30}. These observations on inhibitory effect of the AgNPs are similar to the above mechanism of inhibitory action of silver ions on microorganisms reported by other researchers.

Antifungal Activity of AgNPs

Antifungal activity of the starch stabilized AgNPs was studied by observing the growth profile of the fungi and by the colony count method. Reported MIC values of AgNPs are higher than this report moreover antifungal activity was checked by agar well

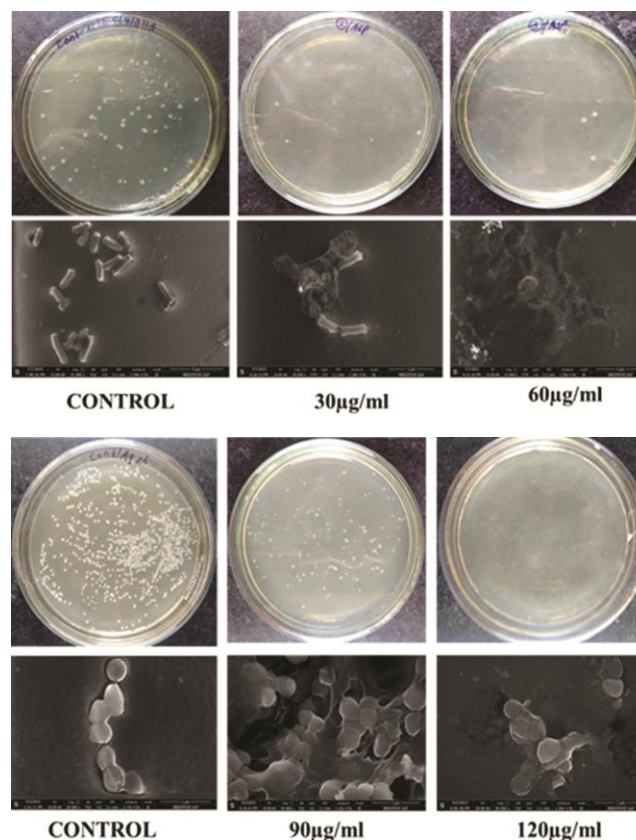


Fig. 8 (A) — Scanning Electron Microscopy of *E. coli*. (B) — Scanning Electron Microscopy of *S. aureus*.

diffusion method in most of the literatures and zone of inhibition was measured³¹⁻³². This report revealed that starch stabilized AgNPs are more prominent against *A. niger* which is observed by spread plate method to check the cell viability and is confirmed by dry weight method. The percentage of inhibition was calculated by counting the colonies in both the NPs treated samples and the corresponding controls. MIC value of AgNPs for *A. niger* was found to be 90 $\mu\text{g/ml}$. Raji *et al* showed anti-fungal activity of starch stabilized AgNPs was 5 mg/ml by *Candida albicans*³³. Growth profile of *A. niger* showed that the fungal cells were able to grow at lower concentration of the NPs (30 and 60 $\mu\text{g/ml}$), but the growth of the treated mycelia was found to be retarded (Fig. 9) as compared to control mycelia. However at the higher AgNPs concentrations (> no growth of the treated cells was observed, even after 48 h of incubation.

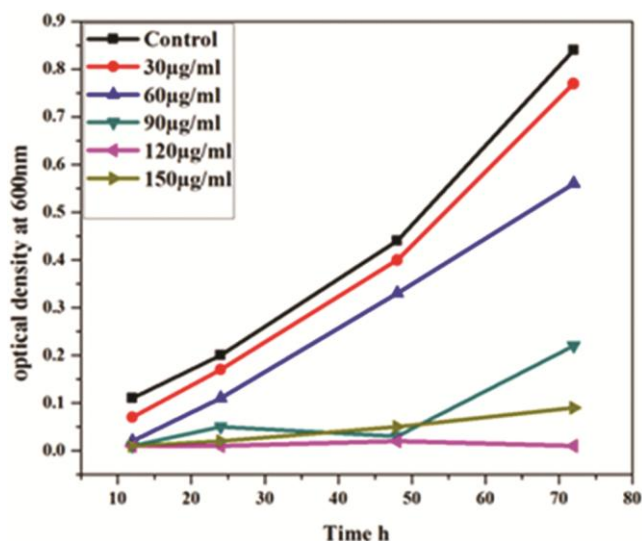


Fig. 9 — Growth profile of *A. niger* in presence of silver nanoparticles.

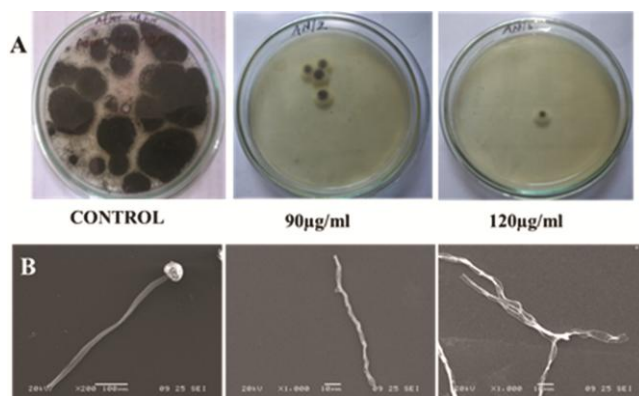


Fig. 10 — Colony count of *Aspergillus niger* and scanning electron microscopy of *A. niger*.

Cell Viability Test

Cells treated with different concentrations of nanoparticles in liquid media were incubated at 37°C for 48 h and controls were run simultaneously. These treated and untreated cells were then plated on PDA plates and kept for incubation at 37°C for 24 h. As seen in Figure 10, in the treated cells an appreciable decrease in the number of colonies was observed as the concentration of AgNPs (60, 90 and 120 $\mu\text{g/ml}$) was increased. A decrease in the diameter of colonies as compared to control was also observed in all treated fungi cells. In fact, at a concentration of 120 $\mu\text{g/ml}$ of the AgNPs only one small fungal colony was found after 48 h of incubation, suggesting almost 100% inhibition of *A. niger*.

As seen in Fig. 9 & 10, morphological changes observed after the treatment of AgNPs, the control fungal mycelia showed a characteristic morphology with round apical head, elongated with a constant diameter and smooth surface of the hyphae. The AgNPs (90 $\mu\text{g/ml}$) treated *A. niger* mycelia were found to be completely distorted in structure with budding of hyphae and distortion of apical tip as compared to control.

Dry weight of mycelia obtained after 7 days of incubation in PDB in absence and in presence of varying concentrations of AgNPs. A marked reduction in dry weight of mycelia treated with the AgNPs was observed as compared to the control. It clearly demonstrates that AgNPs acting as a fungicidal to inhibited the growth of *A. niger*.

Cytotoxic Assay

The HeLa cells were treated with AgNPs (6.2 μg to 200 $\mu\text{g/ml}$) concentrations for 24 h. No significant

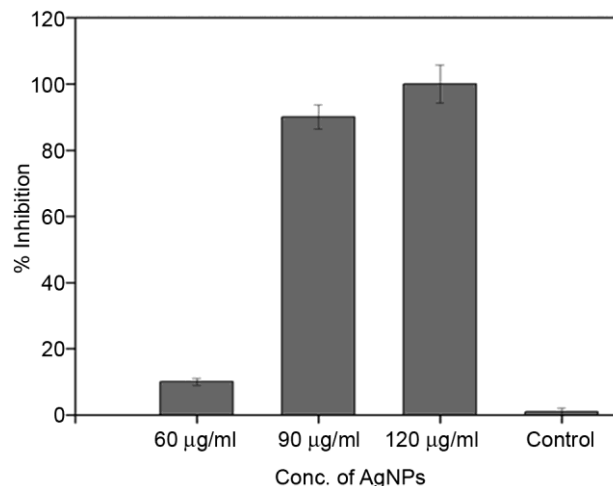


Fig. 11 — Dry weight of *A. niger* after treatment of AgNPs.

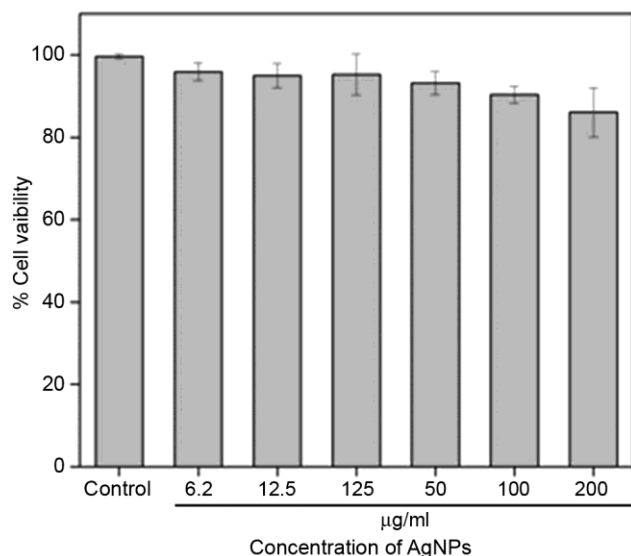


Fig. 12 — Cytotoxicity of AgNPs on HeLa cell lines by MTT assay.

change in cell viability was observed at lower concentrations as compared to control. AgNPs at higher concentration (200 µg/ml) showed cell viability around 86% (Fig. 12). Cytotoxicity of starch stabilized AgNPs against HeLa cell lines by the MTT assay, which relies on the fact that metabolically active cells reduce MTT to purple formazan. Hence, the intensity of dye read at 570 nm is directly proportional to the number of viable cells. The cell viability results suggest that the green synthesized starch stabilized silver nanoparticles are non-toxic to the HeLa cell lines tested. AgNPs exerted no significant cytotoxic effect at 200 µg/ml which is 100% lethal for bacteria and fungi. MIC values found against bacteria, *E. coli* and *S. aureus*, were 60 µg/mL and 120 µg/ml, and 90 µg/ml MIC was observed for *A. niger*.

Conclusion

Green synthesis of silver nanoparticles was carried out using starch (isolated from *F. esculentum* seeds in our laboratory) as a capping and reducing agent. At pH 8 nanoparticles showed yellow color and surface plasmon resonance absorption peak at 418 nm. This study revealed that the 20-30 nm average sized AgNPs had excellent antibacterial action against bacteria. The nanoparticles also exhibited antifungal activity against the fungus *A. niger* and AgNPs are non-toxic to the human cell lines (HeLa cell lines) were confirmed by MTT assay.

Acknowledgments

Authors are grateful to Uniiversity Grant Commission-BSR, New Delhi, India meritorious

fellowship for financial support and Department of Chemistry, SPPU, Pune, India for providing facilities to carry out this work.

References

- Vidhu V K, Aromal S A & Philip D, Green synthesis of silver nanoparticles using *Macrotyloma uniflorum*, *Spectro Acta Part A*, 83 (2011) 392–39, doi:10.1016/j.saa.2011.08.051⁽²⁰⁰³⁾.
- Poovathinthodiyil R, Fu J & Wallen S L, Completely green synthesis and stabilization of metal nanoparticles, *J Am Chem Soc*, 125 13940–13941.
- Ayala V G, Oliveira Vercik L C, Ferrari R & Vercik A, Synthesis and characterization of silver nanoparticles using water-soluble starch and its antibacterial activity on *Staphylococcus aureus*, *Starch/Stärke*, 65 (2014) 931–937, doi.org/10.1021/ie4030903.
- Szymońska J, Targosz-Korecka M & Krok F, Characterization of starch nanoparticles, *J Phys: Conference Series*, 46 (2009) 12-27, doi:10.1088/1742-6596/146/1/012027.
- Chung Y C, Chen I H & Chen C J, The surface modification of silver nanoparticles by phosphoryl disulfides for improved biocompatibility and intra cellular uptake, *Biomater*, 29 (2008) 1807–1816, doi:10.1016/j.biomaterials.2007.12.032.
- Corre D L, Bras J & Dufresne A, Starch nanoparticles: A review, *Biomacro*, 11 (2010) 1139–1153.
- Bose D & Chatterjee S, Antibacterial activity of green synthesized silver nanoparticles using vasaka (*Justicia adhatoda* L.) leaf extract, *Indian J Microb*, 55 (2015) 163–167, doi:10.1007/s12088-015- 0512-1.
- Skrabanja V, Laerke H N & Krefit I, effects of hydrothermal processing of buckwheat (*Fagopyrum esculentum* Moench) groats on starch enzymatic availability *in vitro* and *in vivo* in rats, *J Cereal Sci*, 28 (1998) 209–214.
- LuD, R, Xiao C M & Xu S J, Starch-based completely biodegradable polymer materials, *eXPRESS Poly Lett*, 3 (2009) 366–375.
- Pal S, Tak Y K & Song J M, Does the antibacterial activity of silver nanoparticles depend on the shape of the nanoparticle? A study of the Gram-negative bacterium *Escherichia coli*, *Appl Environ Micro*, 73 (2007) 1712–1720, doi:10.1128/AEM.02218-06.
- Morones J R, Elechiguerra J L, Camacho A, Holt K, Kouri J B *et al*, The bactericidal effect of silver nanoparticles, *Nanotechnol*, 16 (2005) 2346-2353, doi:10.1088/0957-4484/16/10/059.
- Vigneshwaran N, Nachane R P, Balasubramanya R H & Varadarajan P V, A novel one-pot ‘green’ synthesis of stable silver nanoparticles using soluble starch, *Carb Res*, 341 (2006) 2012-2018, doi:10.1016/j.carres.2006.04.042.
- Sharm N & Tripathi A, Effects of *Citrus sinensis* (L.) Osbeck epicarp essential oil on growth and morphogenesis of *Aspergillus niger* (L.) Van Tieghem, *Microbiol Res*, 163 (2008) 337-344, doi:10.1016/j.micres.2006.06.009.
- Ghosh S, Kaushik R, Nagalakshmi K, Hoti S L, Menezes G A *et al*, Antimicrobial activity of highly stable silver nanoparticles embedded in agar-agar matrix as a thin film, *Carb Res*, (2010) 345, 2220–2227, doi:10.1016/j.carres.2010.08.001.
- Harada M, Inada Y & Nomura M, *In situ* time-resolved

- XAFS analysis of silver particle formation by photo reduction in polymer solutions, *J Coll Int Sci*, 337 (2009) 427–438. doi:10.1016/j.jcis.2009.05.035.
- 16 Rastogi L, Sashidhar R B, Karunasagar D & Arunachalama J, Gum kondagogu reduced/stabilized silver nanoparticles as direct colorimetric sensor for the sensitive detection of Hg²⁺ in aqueous system, *Talanta*, 11 (2013) 111–118, doi.org/10.1016/j.talanta.2013.10.012.
- 17 Tagada C K, Reddy Dugasanic S, Aiyer R, Park S, Kulkarni A *et al*, Green synthesis of silver nanoparticles and their application for the development of optical fiber based hydrogen peroxide sensor, *Sen Act B*, 183 (2013) 144–149, doi.org/10.1016/j.snb.2013.03.106.
- 18 Khana Z, Singha T, Hussaina J I, Obaid A. Y, AL-Thabaiti S A & Mossalamy E H, Starch-directed green synthesis, characterization and morphology of silver nanoparticles, *Coll Surf B: Biointerfaces*, 102 (2013) 578–584.
- 19 Velmurugan P, Hydroose M, Lee S M, Cho M, Park J H *et al*, Synthesis of silver and gold nanoparticles using cashew nut shell liquid and its antibacterial activity against fish pathogens, *Indian J Microbiol*, 54 (2014) 196–202, doi.10.1007/s12088-013-0437-5.
- 20 Raghavendra G M, Jung J, Kim D & Seo J, Step-reduced synthesis of starch-silver nanoparticles, *International J Biol Macro*, 86 (2016), 126–128.
- 21 Kora A J, Beedu S R & Jayaraman A, Size-controlled green synthesis of silver nanoparticles mediated by gum ghatti (*Anogeissus latifolia*) and its biological activity, *Org Med Chem Lett*, 2 (2012) 1-10.
- 22 Durán N, Cuevas R, Cordi L, Rubilar O & Diez M C, Biogenic silver nanoparticles associated with silver chloride nanoparticles (Ag@AgCl) produced by laccase from *Trametes versicolor*, *Spr Plus*, 3 (2014) 645.
- 23 Erjaee H, Rajaian H & Nazifi S, Synthesis and characterization of novel silver nanoparticles using *Chamaemelum nobile* extract for antibacterial application, *Adv Nat Sci: Nanosci Nanotech*, 8 (2017) 1-9.
- 24 Zhang Yu, Yang Mo, Portney N G, Cui D, Budak G *et al*, Zeta potential: A surface electrical characteristic to probe the interaction of nanoparticles with normal and cancer human breast epithelial cells, *Biomed Microdevi*, 10 (2008) 321–328.
- 25 Feng Q L, Wu J, Chen G Q, Cui F Z, Kim T N *et al*, A mechanistic study of the antibacterial effect of silver ions on *Escherichia coli* and *Staphylococcus aureus*, *J Biomed Mat Res*, 52 (2000) 662-668.
- 26 Shrivastava S, Bera T, Roy A, Singh G, Ramachandrarao P *et al*, Characterization of enhanced antibacterial effects of novel silver nanoparticles, *Nanotec*, 18 (2007) 103-225.
- 27 Raffi M, Hussain F, Bhatti T M, Akhter J I, Hameed A *et al*, Antibacterial characterization of silver nanoparticles against *Escherichia Coli* ATCC 15224, *J Mat Sci Technol*, 24 (2008) 192-196.
- 28 Sondi I and Salopek-Sondi B, Silver nanoparticles as antimicrobial agent: A case study on *Escherichia coli* as a model for Gram-negative bacteria, *J Coll Int Sci*, 275 (2004) 177–182, doi:10.1016/j.jcis.2004.02.012.
- 29 Thombre, Chitnis R, Kadam A, Bogawat Y, Rochelle C *et al*, A facile method for synthesis of silver nanoparticles using *Eichhornia crassipes* (Mart.) Solms (water hyacinth), *Indian J Biotech*, 13 (2014) 337-341.
- 30 Rana S & Kalaichelvan P T, Antibacterial activities of metal nanoparticles, *Adv Biotech*, 11 (2011) 21-23.
- 31 Nasrollahi A, Pourshamsian K & Mansourkiaee P, Antifungal activity of silver nanoparticles on some of fungi, *Int J Nano*, (2011) Dim, 233-239.
- 32 Thombre R, Parekh F, Lekshminarayanan P & Francis G, Studies on antibacterial and antifungal activity of silver nanoparticles synthesized using *Artocarpus heterophyllus* leaf extract, *Biotechnol Bioinf Bioeng*, 2 (2012) 632-637.
- 33 Raji V, Chakraborty M & Parikh P A, Synthesis of starch-stabilized silver nanoparticles and their antimicrobial activity, *Part Sci Tech*, 30 (2012) 565–577.